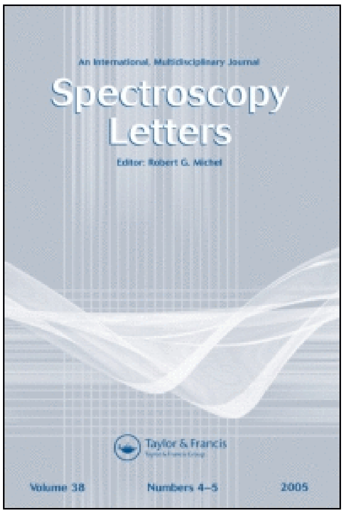

Spectroscopy Letters
Publication details, including instructions for authors and subscription information:
http://www.informaworld.com/smpp/title~content=t713597299

Solvent-Assisted Self-Quenching of the $^5D_3$-State of Tb^3 in $POCl_3$:$SnCl_4$

J. Chrysochoos[a]
[a] Department of Chemistry, University of Toledo, Toledo, Ohio

To cite this Article Chrysochoos, J.(1980) 'Solvent-Assisted Self-Quenching of the $^5D_3$-State of Tb^3 in $POCl_3$:$SnCl_4$', Spectroscopy Letters, 13: 12, 847 — 859
To link to this Article: DOI: 10.1080/00387018008064072
URL: http://dx.doi.org/10.1080/00387018008064072

SPECTROSCOPY LETTERS, 13(12), 847-859 (1980)

SOLVENT-ASSISTED SELF-QUENCHING OF THE $^5D_3$-STATE OF Tb^{3+} in $POCl_3$:$SnCl_4$

J. Chrysochoos

Department of Chemistry
University of Toledo
Toledo, Ohio 43606

ABSTRACT

The near infrared and visible spectra of Tb^{3+} in $POCl_3$:$SnCl_4$, in conjunction with the corresponding emission spectra, reveal an energy mismatch between the nonradiative transitions $^5D_3 \rightarrow {}^5D_4$ and $^7F_0 \leftarrow {}^7F_6$ in favor of the former. This energy mismatch increases at higher temperatures. The temperature dependence of the self-quenching of the $^5D_3$-state of Tb^{3+}, which requires the coupling between the aforementioned transitions, can be accounted for via a mode-assisted process.

INTRODUCTION

Excitation of Tb^{3+} in crystals with near UV light gives rise to two groups of emission bands arising from both the $^5D_3$ and $^5D_4$-states of Tb^{3+}.(1-3) The $^5D_3$-state undergoes electronic relaxation via a process assisted by adjacent Tb^{3+}-ions.(4)

The fluorescence of Tb^{3+} in aqueous solutions and in organic solvents arises exclusively from the $^5D_4$-state (5-9) due to a very effective electronic relaxation of the $^5D_3$-state. On the other hand, light excitation by Tb^{3+} in aprotic solvents such as $POCl_3$:$SnCl_4$ with $\lambda < 380$ nm, gives rise to emission arising from both the $^5D_4$ and the $^5D_3$-states.(10-12) The electronic relaxation of the $^5D_3$-state in such systems has been studied as a function of the temperature, $[Tb^{3+}]$, and solvent composition.(10-12) The self-quenching process of the $^5D_3$-state of Tb^{3+} is temperature dependent,

$$Tb^{3+}(^5D_3) + Tb^{3+}(^7F_6) \rightarrow Tb^{3+}(^5D_4) + Tb^{3+}(^7F_j);\ kq \qquad (1)$$

associated with an activation energy barrier of 3.0 kcal/mole.(10) The quenching rate constant (k_s) of the $^5D_3$-state interacting with the solvent, was found to be in the range of 600-800 sec^{-1}.(13)

The temperature dependence of the self-quenching process of the $^5D_3$-state of Tb^{3+} is not clear. The near infrared spectra of Tb^{3+} were studied to determine the energy of the ground state manifold of Tb^{3+} in $POCl_3$:$SnCl_4$ and to elucidate the dynamics of the coupling between the radiationless transitions $^5D_3 \rightarrow {}^5D_4$ and $^7F_j \leftarrow {}^7F_6$.

EXPERIMENTAL

Terbium chloride, $TbCl_3 \cdot 6H_2O$, of 99.9% to 99.99% purity was converted to anhydrous $TbCl_3$ and dissolved in appropriate mixtures of $POCl_3$ and $SnCl_4$ under refluxing conditions in the absence of H_2O and CO_2. Near infrared spectra were recorded with a Cary-14 Spectrophotometer. Emission spectra were obtained with an Aminco-Bowman Spectrophotofluorimeter. Experimental details can be found elsewhere.(10-12)

RESULTS AND DISCUSSION

A typical near infrared spectrum of Tb^{3+} in $POCl_3$:$SnCl_4$ is illustrated in Figure 1. The spectrum was recorded using $POCl_3$:$SnCl_4$ under otherwise identical conditions. The near infrared spectrum extends from 1700 nm to 2500 nm. The spectral region beyond 2550 nm is masked by the absorption of $POCl_3$:$SnCl_4$. The absorption bands of Tb^{3+} attributed to the transitions $^7F_{4,5} \leftarrow {}^7F_6$ are not shown because they appear at wavelengths longer than 2600 nm. The spectrum illustrated in Figure (1) shows clearly the absorption bands attributed to the transitions $^7F_3 \leftarrow {}^7F_6$, $^7F_2 \leftarrow {}^7F_6$ and $^7F_1 \leftarrow {}^7F_6$. The absorption band due to the $^7F_0 \leftarrow {}^7F_6$-transition is less distinct, because it is masked by the broad absorption band due to $^7F_1$-state.

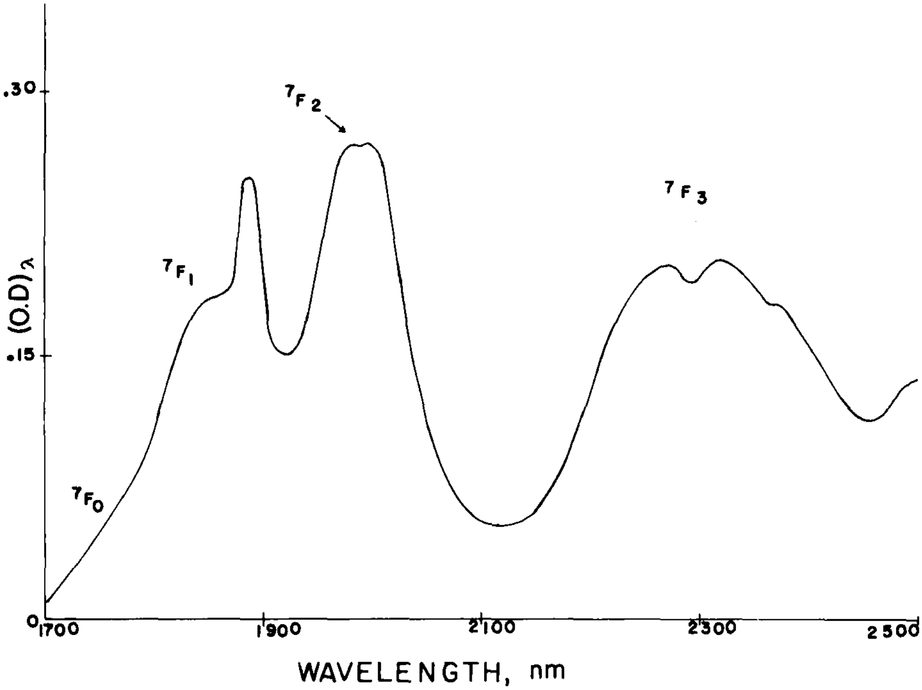

Figure 1. Near infrared absorption spectrum of 5 x 10^{-4}M Tb^{3+} in $POCl_3$:$SnCl_4$ 10:1 (V/V) vs $POCl_3$:$SnCl_4$ 10:1 (V/V); Room T; L = 5.00 cm

All the absorption bands shown in Figure 1 obey Beer's Law. Some of these plots are depicted in Figure 2 under different experimental conditions. An absorption band which appears at about 2600 nm does not obey Beer's Law; it is virtually independent of [Tb^{3+}] and it is attributed to the solvent.

The near infrared spectrum of Tb^{3+} exhibits a slight temperature dependence. In general, at higher temperatures, part of the spectrum shift to slightly lower energies (Figure 3). However, this shift is very gradual and not very distinct. The slight temperature dependence of the near infrared spectrum is illustrated more clearly in Figure 4 in which the optical density at several wavelengths is plotted against the temperature.

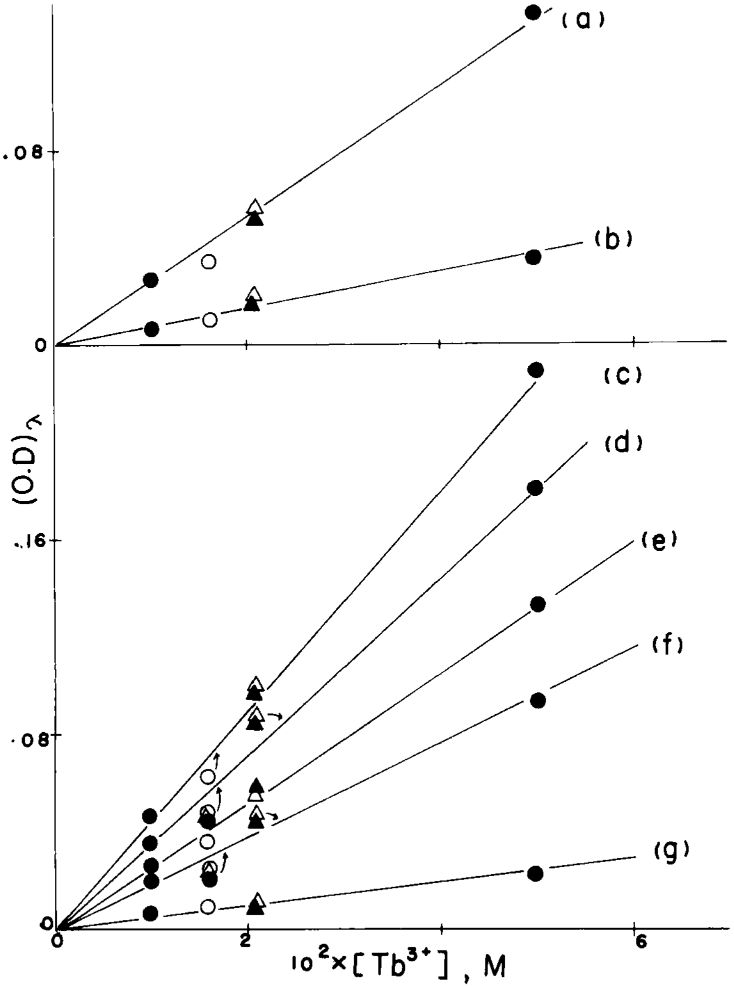

Figure 2. Beer-Lambert Plots of Tb^{3+} in $POCl_3$:$SnCl_4$; Room T: L = 5.00 cm. (a) 2320 nm (b) 2160 nm (c) 1980 nm (d) 1885 nm (e) 2260 nm (f) 1820 nm and (g) 1740 nm
○ $POCl_3$:$SnCl_4$ 10:1 (V/V); ● $POCl_3$:$SnCl_4$ 11.5:1 (V/V); ▲ $POCl_3$:$SnCl_4$ 14.6:1 (V/V); △ $POCl_3$:$SnCl_4$ 24:1 (V/V)

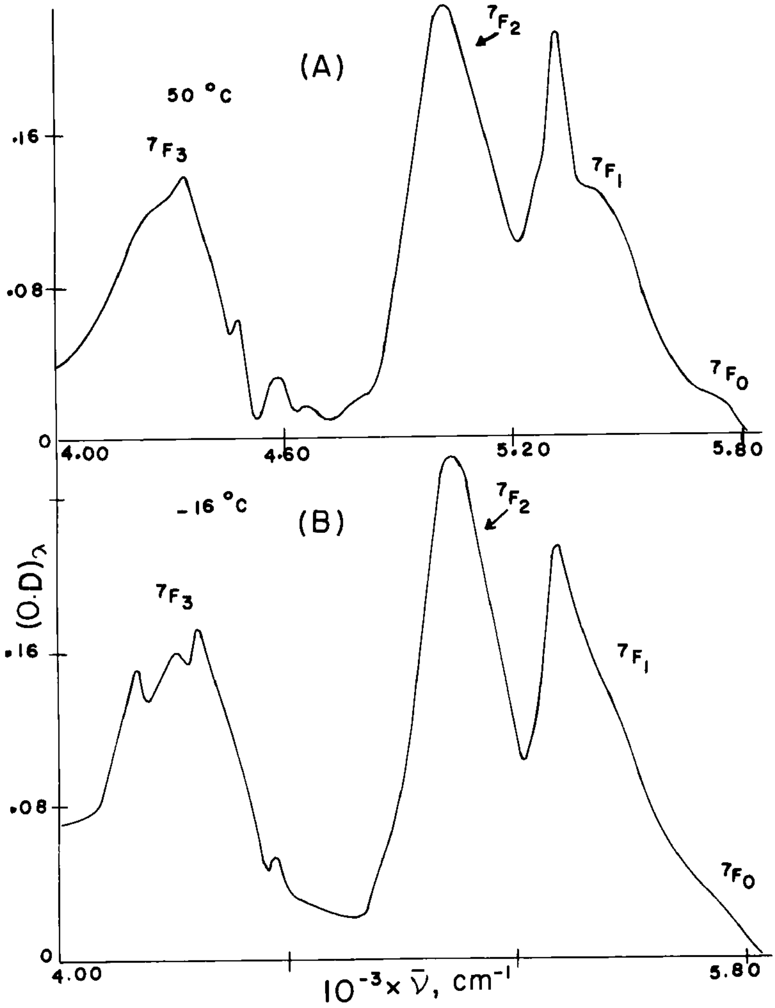

Figure 3. Near infrared absorption spectrum of 5 x 10^{-2}M Tb^{3+} in $POCl_3$:$SnCl_4$ 10:1 (V/V); L = 5.00 cm; Reference, $POCl_3$:$SnCl_4$ 10:1 (V/V). (A) 50°C (B) -16°C

To eliminate the effect of changes in the concentration of Tb^{3+} due to the thermal expansion of the solvent, the ratio $(O.D)_\lambda/(O.D)_{370}$ instead of $(O.D)_\lambda$, was plotted vs. the temperature, where $(O.D)_{370}$ is the optical density of a narrow and relatively intense absorption band of Tb^{3+} in the

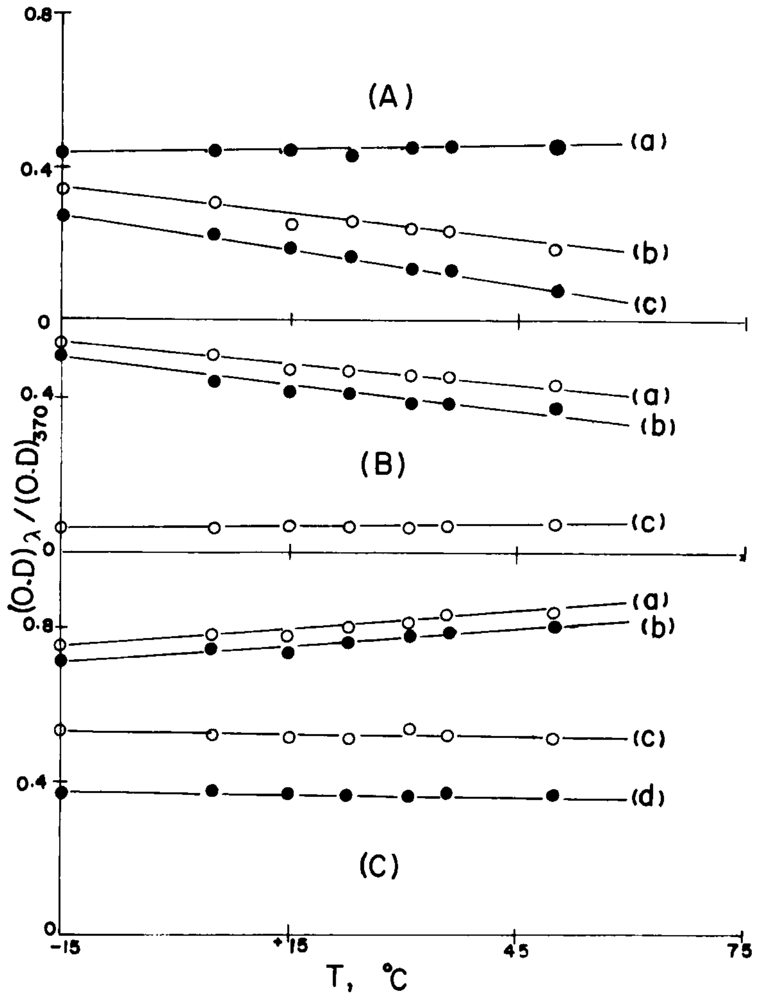

Figure 4. Variations of $(O.D)_\lambda/(O.D)_{370}$ with the temperature; 5×10^{-2}M Tb^{3+} in $POCl_3$:$SnCl_4$ 10:1 (V/V); L = 5.00 cm. (A) $^7F_3 \leftarrow {}^7F_6$-transition (a) 2370 nm (4220 cm^{-1}) (b) 2230 nm (4484 cm^{-1}); (c) 2220 nm (4504 cm^{-1}). (B) $^7F_2 \leftarrow {}^7F_6$-transition. (a) 1980 nm (5050 cm^{-1}); (b) 1970 nm (5076 cm^{-1}); (c) 2030 nm (4926 cm^{-1}). (C) $^7F_1 \leftarrow {}^7F_6$-transition; (a) 1880 nm (5319 cm^{-1}); (b) 1885 nm (5305 cm^{-1}); (c) 1850 nm (5405 cm^{-1}); (d) 1800 nm (5555 cm^{-1}).

near UV spectral region. In part (A) of Figure 4 the optical density at 2370 nm (4220 cm^{-1}) exhibits a slight increase with increasing temperature whereas the optical densities at 2230 nm (4484 cm^{-1}) and 2220 nm (4504 cm^{-1}) decrease slightly. These three wavelengths correspond to different components of the absorption envelope attributed to the $^7F_3 \leftarrow {}^7F_6$ transition of Tb^{3+}. The lower energy component gains intensity at the expense of the higher energy components at higher temperatures. In part (B) of Figure 4 the optical densities at 1980 nm (5050 cm^{-1}) and 1970 nm (5076 cm^{-1}) decrease slightly at higher temperatures whereas the optical density at 2030 nm (4926 cm^{-1}) gains very slightly. These wavelengths correspond to components of the absorption envelope attributed to the $^7F_2 \leftarrow {}^7F_6$-transition. Similarly, in part (C) of Figure 4, which illustrates components of the absorption envelope attributed to the $^7F_1 \leftarrow {}^7F_6$-transition, the optical densities at 1880 nm (5319 cm^{-1}) and 1885 nm (5305 cm^{-1}) clearly increase with increasing temperature whereas the optical densities at 1850 nm (5405 cm^{-1}) and 1800 nm (5555 cm^{-1}) are virtually temperature independent.

Energy parameters of the near infrared absorption bands and the emission bands of Tb^{3+} in $POCl_3:SnCl_4$ are given in Table I. The energy gap, ΔE_1, between the $^5D_3$ and $^5D_4$-states of Tb^{3+} in $POCl_3:SnCl_4$, determined from the emission maxima, namely

$$\Delta E_1 = E(^5D_3) - E(^5D_4) = \bar{\nu}_{max}(^5D_3 \rightarrow {}^7F_J) - \bar{\nu}_{max}(^5D_4 \rightarrow {}^7F_J)$$

varies with the temperature. The corresponding average values of ΔE_1, determined from four pairs of emission bands, were found to be 5747 cm^{-1} at 55°C and 5679 cm^{-1} at -16°C. Similar values were obtained from the absorption spectra of Tb^{3+}

$$\Delta E_2 = E(^5D_3 \leftarrow {}^7F_6) - E(^5D_4 \leftarrow {}^7F_6)$$

Values of ΔE_2 determined in this way are 5770 cm^{-1} at 55°C and 5664 cm^{-1} at -16°C. In addition, the energy difference between the highest and the lowest energy components of the ground state manifold, ΔE_3 is about 5720 cm^{-1} at -16°C and less than 5720 cm^{-1} at 55°C.

TABLE I

Energy parameters of the near infrared absorption and emission bands of Tb^{3+} in $POCl_3$:$SnCl_4$ at -16°C

Transition	$\bar{\nu}_{max}$ (cm^{-1})		$(\Delta\bar{\nu})_{1/2}$	$E(^5D_3) - E(^5D_4)$
	Absorption	Emission	cm^{-1}	cm^{-1}
$^7F_3 \leftarrow {}^7F_6$	4360	--	380	
$^7F_2 \leftarrow {}^7F_6$	5020; 5310	--	$\sim$300	
$^7F_1 \leftarrow {}^7F_6$	5460	--	--	
$^7F_0 \leftarrow {}^7F_6$	5720	--	--	
$^5D_4 \leftarrow {}^7F_6$	20533	--	250	5782
$^5D_3 \leftarrow {}^7F_6$	26315	--	$\sim$200	
$^5D_3 \rightarrow {}^7F_6$	--	25974	$\sim$500	5732
$^5D_4 \rightarrow {}^7F_6$	--	20242	$\sim$500	
$^5D_3 \rightarrow {}^7F_5$	--	23866	$\sim$500	5618
$^5D_4 \rightarrow {}^7F_5$	--	18248	$\sim$360	
$^5D_3 \rightarrow {}^7F_4$	--	22675	$\sim$400	5640
$^5D_4 \rightarrow {}^7F_4$	--	17035	$\sim$370	
$^5D_3 \rightarrow {}^7F_3$	--	21691	$\sim$350	5666
$^5D_4 \rightarrow {}^7F_3$	--	16025	--	
$^5D_3 \rightarrow {}^7F_2$	--	21141	$\sim$300	
$^5D_3 \rightarrow {}^7F_1$	--	20576	--	

From these values one obtains:

$$\Delta E = \Delta E_1 - \Delta E_3 > 50 \text{ cm}^{-1}$$

The value of ΔE increased further with increasing temperature. This value represents the energy mismatch between the transitions which have to be coupled to lead to the self-quenching of the $^5D_3$-state of Tb^{3+}.

$$Tb^{3+}(^5D_3) + Tb^{3+}(^7F_6) \rightarrow Tb^{3+}(^5D_4) + Tb^{3+}(^7F_0) + \Delta E \qquad (2)$$

Under these conditions the efficiency of process (2) should increase at lower temperatures. This is just the opposite of what has been observed experimentally. Process (2) is associated with an activation energy barrier equal to 3.0 kcal/mole.(10)

If the lowest energy component of the ground state multiplet ($^7F_6$) is arbitrarily taken as zero, the average energies of the remaining components of the multiplet can be estimated from the absorption and emission spectra,

$$E(^7F_j) = ([E(^5D_4 \leftarrow {}^7F_6) - E(^5D_4 \rightarrow {}^7F_j)] + [E(^5D_3 \leftarrow {}^7D_6) - E(^5D_3 \rightarrow {}^7F_j)])/2 \qquad (3)$$

Such energy estimates are summarized in Table II along with appropriate literature values. It is apparent in the case of Tb^{3+} in $POCl_3$:$SnCl_4$ that

$$E(^5D_3) - E(^5D_4) > E(^7F_0) - E(^7F_6)$$

Therefore, the electronic relaxation of the $^5D_3$-state of Tb^{3+} via the ground state manifold of an adjacent Tb^{3+}-ion involves the dissipation of an excess energy. This energy appears to be taken up by the solvent (s)

$$Tb^{3+}(^5D_3) + Tb^{3+}(^7F_6) + s(v{=}o) \rightarrow Tb^{3+}(^5D_4) + Tb^{3+}(^7F_j) + s(v{\neq}o) \qquad (4)$$

Both the amount of energy which must dissipate and the efficiency of process (4) increase at higher temperatures. It is possible that at higher temperatures the solvation sphere of Tb^{3+} becomes distorted and the

TABLE II

Energy levels of Tb^{3+} in $POCl_3:Cl_4$ at -16°C

$\bar{\nu}(cm^{-1})$

Level	Absorption	$\Delta\bar{\nu}$	Emission & Absorption	$\Delta\bar{\nu}$	Tb^{3+} in LaF_3(14)		$\Delta\bar{\nu}$	TbF_3(15) at 20 K
					Observed	Calculated		
$^7F_6$	Zero(Arbitrary)		∼315		-	124		0-488
				2052			2048	
$^7F_5$	-		2367 ± 80			2172		2139-2357
				1202			1267	
$^7F_4$	-		3569 ± 80			3439		3366-3667
				997			979	
$^7F_3$	4360		4566 ± 60		4423	4418		4455-4598
		660		608			188	
$^7F_2$	5020		5174		5074	5106		5109-5289
		290;440		565			455	
$^7F_1$	5310; ∼5460		5739		5560	5561		5606-5801
		410;260		-			223	
$^7F_0$	∼5720		-		5814	5784		5945
		14813		-			14784	
$^5D_4$	20533		-		-	20568		20603-20721
		5782		-			5782	
$^5D_3$	26315		-		-	26360		-
		-		-				-

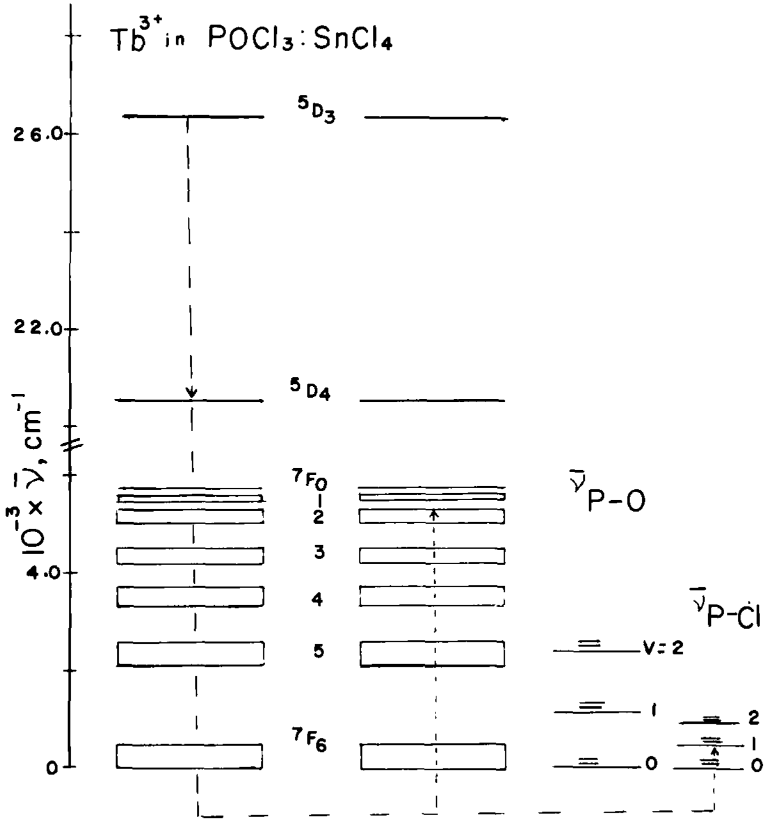

Figure 5. Energy level diagram of Tb^{3+} in $POCl_3$:$SnCl_4$ (ground state multiplet and low excited states) and vibrational levels (16,17) of the P-O and P-Cl stretching modes of $POCl_3$:$SnCl_4$.

strict selection rules which may control process (4) become partly relaxed, leading to a more efficient self-quenching of the $^5D_3$-state.

Vibrational modes of $POCl_3$ associated with relatively high energy are the P-O stretching mode at 1290 cm^{-1} and the P-Cl stretching mode at 484 and 588 cm^{-1}. (16,17) The frequency of the P-O stretching mode shifts to 1215 cm^{-1} upon the addition of $SnCl_4$. The frequencies of the P-Cl mode on the other hand shift to slightly higher values upon such an addition. These two vibrational modes are the most likely ones to participate in process (4). The energetics of this process are illustrated in Figure 5. The rotational levels inserted in the vibrational level diagrams of the P-Cl and P-O stretching modes are not to scale. It is apparent that without the assistance of these modes the transitions $^5D_3 \rightarrow {}^5D_4$ and $^7F_0 \leftarrow {}^7F_6$ cannot couple nonradiatively. However, in the presence of the aforementioned vibrational stretching modes cooperative energy transfer can take place, at least in principle. The process outlined in Figure 5 is just once of several possible mechanisms via which the $^5D_3$-state of Tb^{3+} can undergo self-quenching in $POCl_3:SnCl_4$.

REFERENCES

1. L. G. Van Uitert and R. R. Soden, J. Chem. Phys., 32, 1161 (1960).
2. K. S. Thomas, S. Singh and G. H. Dieke, J. Chem. Phys., 38, 2180 (1963).
3. N. Rabbiner, J. Opt. Soc. Amer., 55, 436 (1965).
4. L. G. Van Uitert, E. F. Dearborn and J. J. Rubin, J. Chem. Phys., 47, 3653 (1967).
5. J. L. Dropp and M. W. Windsor, J. Chem. Phys., 42, 1599 (1965).
6. N. A. Kazanskaya and E. B. Sveshnikova, Opt. Spectrosc., 29, 376 (1970).
7. E. B. Sveshnikova and V. L. Ermolaev, Opt. Spectrosc., 30, 208 (1971).
8. J. Chrysochoos and A. Evers, Chem. Phys. Lett., 20, 174 (1973).
9. J. Chrysochoos, J. Lumin., 9, 79 (1974).
10. P. Tokousbalides and J. Chrysochoos, Chem. Phys. Lett., 29, 226 (1974).
11. J. Chrysochoos and P. Tokousbalides, J. Lumin., 11, 119 (1975).
12. P. Tokousbalides and J. Chrysochoos, J. Chem. Phys., 64, 1863 (1976).
13. J. Chrysochoos, J. Chem. Phys., 69, 5545 (1978).
14. W. T. Carnall, H. Crosswhite and H. M. Crosswhite, "Energy Level Structure and Transition Probabilities in the Spectra of the Trivalent Lanthanides in LaF_3", Technical Report, Argonne National Laboratory (1977).

15. D. C. Krupka and H. J. Guggenheim, J. Chem. Phys., 51, 4006 (1969).

16. K. Nakamoto, "Infrared Spectra of Inorganic and Coordination Compounds", John Wiley and Son, New York, New York (1963); p. 112.

17. M. E. Peak and T. W. Waddington, J. Chem. Soc., 3450 (1962).

Received: September 27, 1980
Accepted: October 20, 1980